

Imaging of the B2 Glenoid: An Assessment of Glenoid Wear

Journal of Shoulder and Elbow
Arthroplasty
Volume 3: 1–9
© The Author(s) 2019
Article reuse guidelines:
sagepub.com/journals-permissions
DOI: 10.1177/2471549219861811
journals.sagepub.com/home/sea



Jared M Mahyilis, MD¹, Vahid Entezari, MD, MMSc²,
Bong-Jae Jun, PhD², Joseph P Iannotti, MD, PhD², and
Eric T Ricchetti, MD² 

Abstract

Background: Glenohumeral osteoarthritis (OA) carries a spectrum of morphology and wear patterns of the glenoid surface exemplified by complex patterns such as glenoid biconcavity and acquired retroversion seen in the B2 glenoid. Multiple imaging methods are available for evaluation of the complex glenoid structure seen in B2 glenoids. The purpose of this article is to review imaging assessment of the type B2 glenoid.

Methods: The current literature on imaging of the B2 glenoid was reviewed to describe the unique anatomy of this OA variant and how to appropriately assess its characteristics.

Results: Plain radiographs, magnetic resonance imaging, and standard 2-dimensional computed tomography (CT) have all shown acceptable assessments of arthritic glenoids but lack the detailed and highly accurate evaluation of bone loss and retroversion seen with 3-dimensional CT.

Conclusion: Accurate preoperative identification of complex B2 pathology on imaging remains essential in planning and achieving precise implant placement at the time of shoulder arthroplasty.

Keywords

B2 glenoid, biconcave glenoid, glenohumeral arthritis

Date received: 16 April 2019; revised: received 19 May 2019; accepted: 16 June 2019

Introduction

Primary glenohumeral osteoarthritis (OA) is a common cause of shoulder pain, affecting nearly 32% of patients over the age of 60 years.^{1,2} The burden of the disease is comparable to other comorbid medical conditions (eg, myocardial infarction), imparting significant disability on those affected.^{3,4} Similar to primary OA of other major joints, glenohumeral OA is characterized by progressive loss of joint space, osteophyte formation, subchondral sclerosis, and cyst formation within bone; but it also carries a spectrum of wear patterns of the glenoid surface.^{5–7} These morphological variations of OA have been shown to have implication on clinical outcomes and survivorship of shoulder arthroplasty.^{8–12}

The B2 glenoid was formally described in 1999 by Walch et al. as part of his original classification of glenoid morphology seen in glenohumeral OA (Figure 1). A total of 5 glenoid variants, including the B2, were described (A1, A2, B1, B2, and C).⁵ However, this was not the first description of the biconcave glenoid.

Dr Charles Neer initially noted the sloped glenoid morphology and the associated posterior humeral head subluxation of the B2 glenoid in 1982, though he did not fully analyze the glenoid variations of glenohumeral OA.¹³ Walch's detailed description was developed from 2-dimensional (2D) preoperative computed tomography (CT) scans in patients undergoing shoulder arthroplasty.⁵ Of the 113 patients examined in this study, type B glenoids comprised 32% of the population with the B2 glenoid seen in 15% of cases.

¹Department of Orthopedic Surgery, Franciscan Health, Olympia Fields, Illinois

²Department of Orthopaedic Surgery, Orthopaedic and Rheumatologic Institute, Cleveland Clinic, Cleveland, Ohio

Corresponding Author:

Eric T Ricchetti, Department of Orthopaedic Surgery, A-40, Orthopaedic and Rheumatologic Institute, Cleveland Clinic, 9500 Euclid Ave, Cleveland, OH 44195, USA.

Email: ricchee@ccf.org



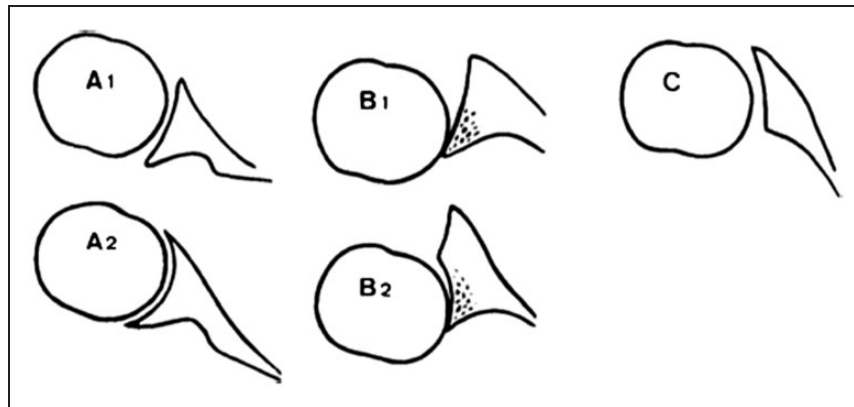


Figure 1. Walch classification of glenoid morphology in primary glenohumeral arthritis (reprinted with permission from Elsevier from Walch et al.⁵).

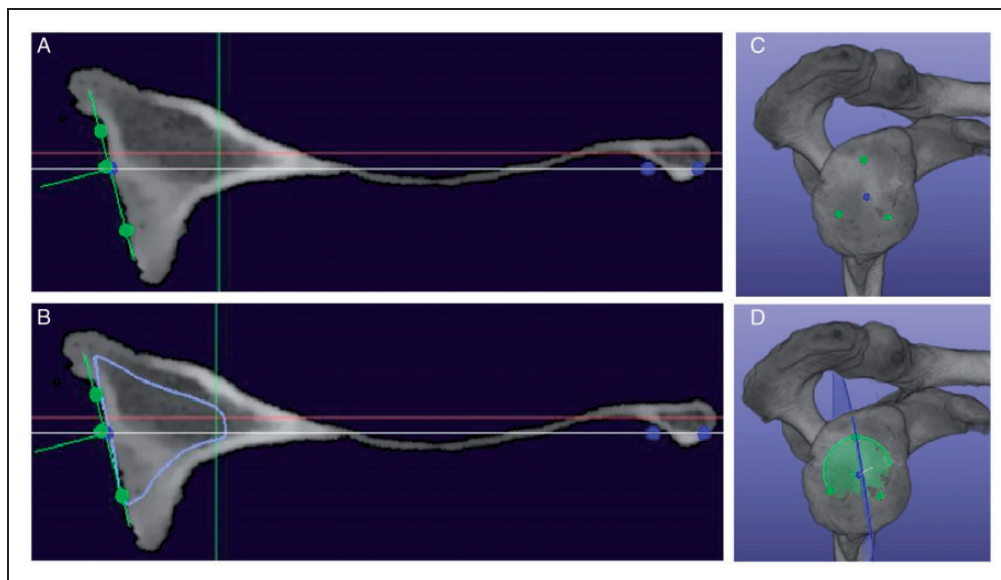


Figure 2. 3D CT of 59-year-old man with B2 glenoid. A, Type B2 glenoid demonstrating pathologic retroversion due to bone loss. Bone measurements: version = -15.9° , inclination = 7.1° . B, Vault model placed in same patient representing pre-morbid glenoid measurements: version = -9° , inclination = 7° . C, 3D reconstruction showing biconcavity. D, 3D reconstruction showing increased retroversion of glenoid plane (green) relative to scapular plane (blue).

Despite the detailed classification, later studies showed agreement between and within surgeons assessing glenoid morphology to be fair to moderate¹⁴ or moderate to substantial,¹⁵ and thus, assessment of glenoid bone loss seen in variants such as the B2 remains challenging. The purpose of this article is to review the radiographic and advance imaging assessment of the B2 glenoid based on the available literature.

The B2 Glenoid: The Biconcave Glenoid

The B2 glenoid (Figure 2) is characterized by biconcavity on the glenoid surface where the native anterior glenoid or paleoglenoid persists and represents preserved

pre-morbid anterior glenoid fossa, while varying amounts of posterior glenoid bone loss occur in association with humeral head translation posteriorly. As the humeral head articulates with the posterior glenoid, this new posterior concavity or neoglenoid is formed. There remains a large spectrum of bone loss in the axial dimension (anterior-posterior) of the biconcavity and depth (medialization) of bone loss may also vary. This arthritic triad (glenoid biconcavity, acquired glenoid retroversion, and humeral head posterior subluxation) presents a significant challenge to address in shoulder arthroplasty.¹⁶

Walch's original description of the B2 noted a "posterior cupula" giving the biconcave appearance along with an average glenoid retroversion of 23.4° for

the B2 and mean posterior humeral head subluxation of 59% for B-type glenoids overall (B1 and B2) when measured relative to the center of the glenoid. Walch felt that subluxation of the humeral head explained the posterior glenoid erosion, which was supported by the symmetric and central erosion of type A glenoids with an absence of subluxation.⁵

The Confounders: The B3 and Other Retroverted Glenoid Variants

Subsequent studies to the original Walch classification revealed challenges with implementation of the classification, even by experienced shoulder surgeons. Scalise et al. showed fair interrater and intrarater agreement in CT analysis of 23 patients with $k = .37$ and $k = .37$, respectively.¹⁴ Nowak et al. showed moderate interobserver ($k = .508$) and substantial intraobserver ($k = .611$) agreement of 26 patient CT scans.¹⁵ Both studies concluded improvements in the classification would provide further utility; thus, the classification has undergone further modification.^{6,7}

Bercik et al. first modified the classification (Figure 3) to report new pathologic glenoid variants and clarify discrepancies of the original Walch classification. One hundred twenty-nine patients with shoulder OA were analyzed by 3-dimensional (3D) CT, in contrast to the original 2D CT study of the Walch classification. They defined a new B3 glenoid variant as monoconcave and posteriorly worn, with at least 15° of retroversion or at least 70% posterior humeral head subluxation relative to

the plane of the scapula, or both. This new highly retroverted variant was felt to occur as a progression from the B2 glenoid, as the paleoglenoid is progressively eroded or by persistent posterior humeral head subluxation preferentially eroding the posterior glenoid without an interval biconcavity.⁶ In a subsequent study, Chan et al. detailed the B3 noting it to be “uniconcave and retroverted. As glenoid retroversion increases, posterior humeral head subluxation significantly increases as referenced to the scapular plane; however, when referenced to the glenoid plane, the head remains concentric to the erosion.”¹⁷ Bercik et al. also clarified the definition of type C glenoid as at least 25° of retroversion due to dysplasia and not caused by posterior erosion so as to address incorrect classification of B2 or B3 glenoids as C glenoids. This modification resulted in improvement of interobserver reliabilities from 0.391 (fair agreement) to 0.703 (substantial agreement) and intraobserver reliabilities from 0.605 (moderate agreement) to 0.882 (nearly perfect agreement).⁶

Further modification of the Walch classification by Iannotti et al. added greater definition to glenoid pathology.⁷ One hundred fifty-five patients with glenohumeral OA were analyzed with 3D CT utilizing previously validated 3D glenoid vault and humeral best-fit circle models to define new glenoid morphologic subtypes. They further defined B3 glenoids as having minimal or no paleo glenoid and high retroversion due to posterior wear, but with significantly more medial wear than a classic B2 glenoid (5.9 ± 2.4 mm joint-line medialization for B3 vs 2.1 ± 1.1 mm for B2, $P < .0001$) and variable

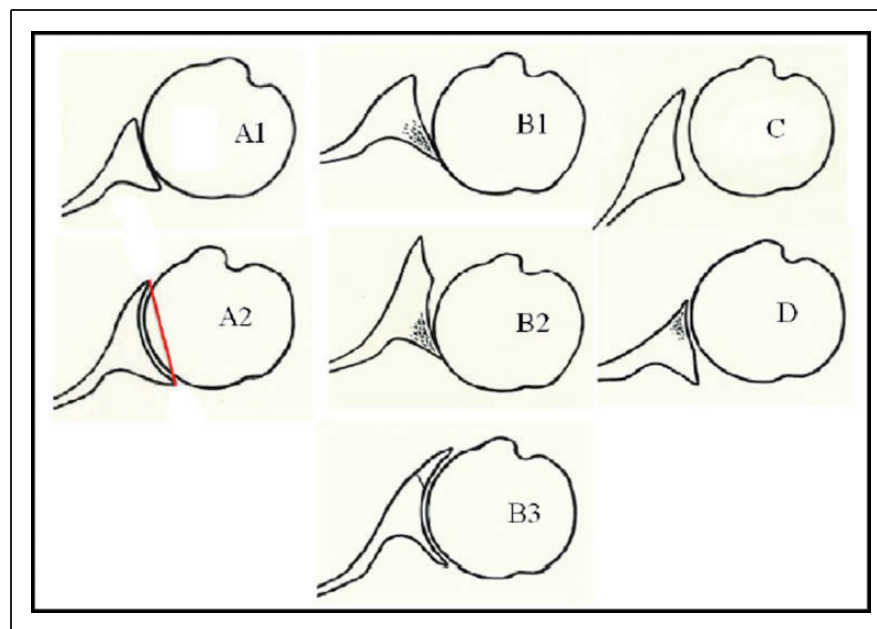


Figure 3. Modified Walch classification. Note that a line drawn from the anterior to posterior native glenoid rim transects the humeral head in A2 glenoid but not in the A1 glenoid (reprinted with permission from Elsevier from Bercik et al.⁶).

posterior humeral head translation, though more frequently the humeral head was centered in the glenoid relative to the subluxated position in B2 glenoids (Figure 4). B3 and B2 glenoids were found to have similar pre-morbid version ($-7.0^\circ \pm 3.2^\circ$ for B3 and $-8.3^\circ \pm 2.8^\circ$ for B2), as measured by the vault model. The C2 glenoid was also introduced. This variant is similar to the B2 glenoid with both biconcavity and posterior

humeral head subluxation present, but with underlying glenoid dysplasia. The C2 was noted to have mean pathologic glenoid retroversion of $-28.5^\circ \pm 4.4^\circ$ compared with $-20.2^\circ \pm 6.6^\circ$ for B2 ($P = .002$) as well as greater pre-morbid glenoid retroversion of $-19.4^\circ \pm 3.3^\circ$ compared to $-8.3^\circ \pm 2.8^\circ$ for B2 ($P < .0001$) (Figure 5). The pre-morbid retroversion in the C2 glenoid was similarly dysplastic to C1, which had a mean of

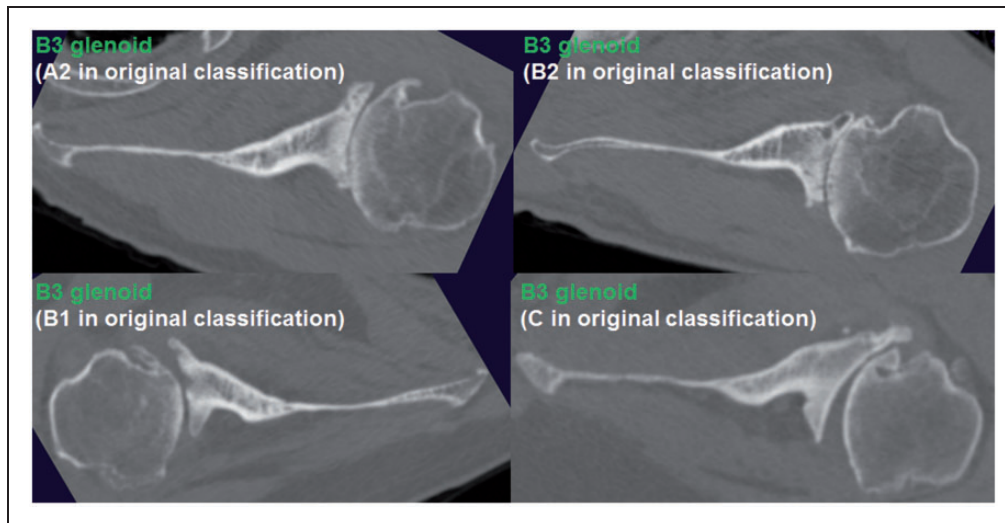


Figure 4. CT scan examples of 4 B3 glenoids and classification according to original Walch classification. Note that the B3 glenoid has both central and asymmetric posterior bone loss, increased medialization, and little to no paleoglenoid unlike the B2 (reprinted with permission from Lippincott Williams & Wilkins from Iannotti et al.⁷).

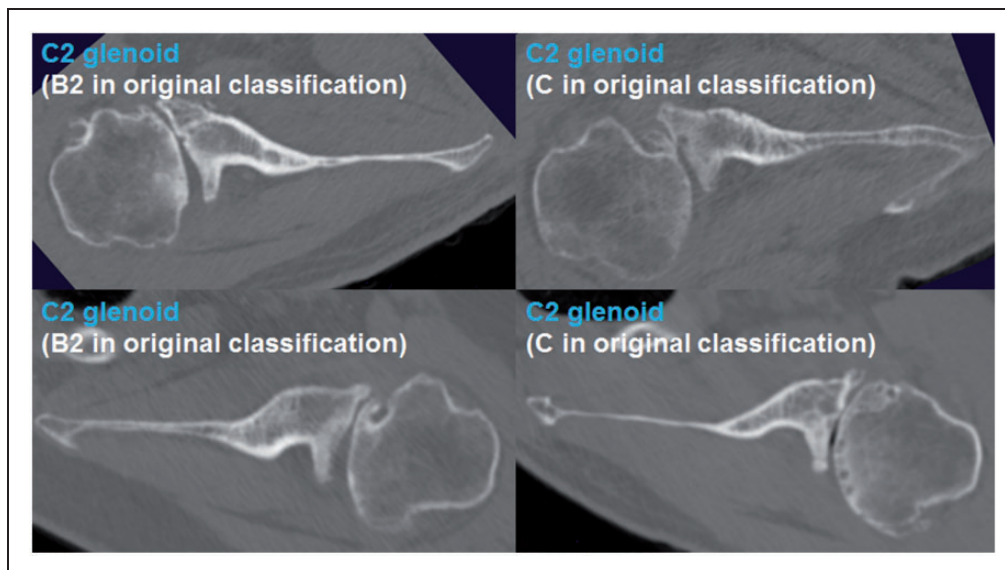


Figure 5. CT scan examples of 4 C2 glenoids and classification according to original Walch classification. In similarity to the B2 glenoid, the C2 glenoid has a biconcave surface with associated posterior humeral head subluxation; however, pathologic glenoid retroversion and the pre-morbid glenoid version are both greater in the C2 glenoid (reprinted with permission from Lippincott Williams & Wilkins from Iannotti et al.⁷).

$-19.0^\circ \pm 8.0^\circ$. The acquired biconcave appearance of the C2 glenoid was associated with greater posterior humeral head subluxation compared with a C1 glenoid, indicating acquired posterior glenoid bone loss in the setting of glenoid dysplasia.⁷

Plain Radiographic Assessment

Although CT was initially used to classify the B2 and other glenoid morphologies,⁵ plain radiographs are often the first images surgeons have to assess the glenoid. Despite its frequency of use, there remain limitations with standard x-rays. Comparing standard axillary x-ray to CT, Nyffeler et al. found that glenoid retroversion was overestimated 86% of the time on plain radiographs with poor interobserver reproducibility on axillary radiographs (coefficient of correlation = .77) and a maximum interobserver difference of up to 35° .¹⁸ More recently, Aronowitz et al. compared axillary radiographs to CT for reliability of assessing the original Walch classification. This study of 75 consecutive shoulders with glenohumeral OA showed intraobserver and interobserver agreement means of $\kappa=0.66$ and $\kappa=0.48$ for plain radiographs and mean $\kappa=0.60$ and $\kappa=0.39$ for CT scans, respectively. The authors concluded that good quality plain axillary radiographs may be sufficient to classify glenoid morphology.¹⁹ In a follow-up to this study, Shukla et al. compared axillary radiographs to CT for reliability of assessing the modified Walch classification. In 100 shoulders with glenohumeral OA, the mean intraobserver and interobserver agreement was $\kappa=0.73$ and $\kappa=0.55$ for plain radiographs and $\kappa=0.72$ and $\kappa=0.52$ for CT scans, respectively. However, the agreement for the 3 surgeons between CT and radiographs after the first read was only 35 of 60 (58%).²⁰

Finally, Kopka et al. compared preoperative axillary x-ray to magnetic resonance imaging (MRI) in 50 patients assessing a 5-category (A1, A2, B1, B2, and C) and a 3-category (A, B, and C) Walch classification. They found moderate interrater x-ray agreement for 5-category ($\kappa=0.42$) and 3-category ($\kappa=0.54$) Walch classifications which was similar to the interrater MRI agreement for both the 5-category ($\kappa=0.47$) and 3-category ($\kappa=0.59$) Walch classifications. The agreement between individual x-ray and consensus MRI readings was much lower: fair-to-moderate for the 5-category ($\kappa=0.21$ – 0.51) and 3-category ($\kappa=0.36$ – 0.60). Interrater agreement for x-ray images was found to be highest for B2 ($\kappa=0.53$) when using the 5-category Walch classifications.²¹

Radiographs exhibit fair to moderate assessment of glenoid pathology for B2 and other morphologies, while CT and MRI have shown more accurate assessment of

pathology and have greater utility for presurgical planning.

Standard 2D CT and 3D CT Assessment

The CT remains the standard for assessment of glenoid morphology since the initial description of the Walch classification and many studies have assessed glenoid morphology based on this modality.^{5,22–28} Identification of the B2 on x-ray and CT remains reliable.^{19,20} However, plain radiographs have notable weakness in assessment of retroversion and degree of bone loss, while CT has shown increased accuracy in assessment of version.¹⁸ 2D glenoid version is most commonly measured by the method of Friedman et al. where a line between the medial border scapular tip and center of the glenoid is referenced for the scapula axis on axial CT.²² A subsequent study by Rouleau et al. confirmed the accuracy of the Friedman method, but also detailed 3 alternate reference lines on the glenoid suitable to assess version of the B2 glenoid (the neoglenoid, the paleoglenoid, and the intermediate glenoid).²³ This study noted the association of the Friedman line for the scapula axis and found the intermediate glenoid line to be the most reliable method for measurement of B2 glenoid version with excellent intraobserver and interobserver reliability (correlation coefficient of greater than 0.957 and 0.954, respectively). A notable weaknesses of version assessment by standard, uncorrected 2D CT, however, relates to the plane of image acquisition and has been seen on multiple studies.^{24,25} Scapular rotation in the coronal and sagittal plane can result in changes in version measurements of up to 10° ,²⁴ and multiple studies have shown increased accuracy in measurement of glenoid pathology with use of 3D CT that corrects the image orientation to the plane of the scapula.^{26,27}

Budge et al. compared standard 2D CT to 3D CT reconstructions in the accuracy of glenoid version measurement. Thirty-four patients were assessed. Three observers measured glenoid version using unmodified mid-glenoid axial cuts on standard 2D CT and using 3D CT reconstructed images corrected to the plane of the scapula with measurements taken in the axial plane. Thirty-five percent of standard 2D measurements were 5° to 10° different and 12% were greater than 10° different from their corresponding 3D corrected CT measurement ($P < .001$ to $P = .045$). Although intraobserver and interobserver reliability was high (0.94–0.98/0.93–0.98 for 2D CT and 0.93–0.96/0.94–0.96 for 3D CT) for 2D and 3D CT, axial 2D images without correction were 5 to 15° different than their 3D corrected counterparts in 47% of measurements.²⁷

Chalmers et al. further showed variations of measured glenoid retroversion with changes of the CT

gantry angle during preoperative assessment specifically of the B2 glenoid. CT analysis of 31 patients with B2 glenoids demonstrated that correction of the 2D CT slice axis to the plane of the scapula resulted in decreased glenoid retroversion by a mean of -2° to -4.7° and a change in glenoid inclination by a mean of 21° ($P < .04$). In 48% of cases, changes in version were $>5^\circ$ and in 94% of cases changes in inclination were $>5^\circ$. This study concluded that CT scans must be reoriented into the plane of the scapula to avoid overestimation of both glenoid version and inclination.²⁶ A second study by this group assessed whether inclusion of the medial border and inferior angle of the scapula is necessary for accurate measurement of glenoid version, inclination, and humeral head subluxation. Fourteen preoperative CT scans in patients with B2 glenoids undergoing total shoulder arthroplasty (TSA) were analyzed for glenoid version, inclination, depth, and humeral head subluxation. Measurements were randomly and blindly repeated after subtracting 12.5%, 25%, and 50% of the scapula from both the medial border and inferior angle. Subtraction of 50% of the scapular width (medial border) resulted in retroversion overestimation by 4.7° , with mean retroversion measurements of 16.5° versus 21.2° for the full scapula and 50% subtracted scapula, respectively ($P = .006$). Inaccuracies in measurement of humeral head subluxation and glenoid depth were also seen when 50% of the scapula was subtracted with overestimations of 2.5% subluxation ($P = .022$) and 0.5 mm depth ($P = .002$). Although exclusion of smaller portions of the medial border or inferior angle did not preclude accurate glenoid measurement, CTs that failed to include 50% of the scapular were recommended to be interpreted with caution.²⁸

Standard 2D CT has shown accurate assessment of glenoid version and glenoid morphology in general, but failure to correct CT scans into the proper scapular orientation or failure to include $>50\%$ of the scapula significantly alters interpretation of glenoid architecture.

3D CT Characteristics of the B2 Glenoid

Advancement in imaging has allowed for more precise assessment of glenoid pathology, and more specifically 3D CT has shown the highest accuracy in defining both premorbid and pathologic glenoid anatomy.^{6,7,27,29-32} As imaging and 3D computer systems have developed so too has our analysis of glenoid wear patterns, especially the B2.

Premorbid anatomy has been shown to be consistent not only between individual patients but also within patients' bilateral anatomy.²⁹⁻³² Knowles et al. evaluated differences in premorbid anatomy with B2 patients specifically. Using 3D CT, they analyzed 80 scapulae, distributed between B2 glenoids and age-matched

normal glenoids. Version and inclination were measured from the anterior paleoglenoid of the B2 glenoids, which served as a premorbid glenoid surrogate, and compared with measurements obtained from similar regions in the normal cohort. They found that the anterior paleoglenoid regions in B2 glenoids were significantly more retroverted ($-14^\circ \pm 6^\circ$) compared with nonarthritic normal glenoids ($-5^\circ \pm 5^\circ$) ($P < .001$). No significant differences were seen between the groups in glenoid inclination ($P = .166$). One notable weakness of the study was the use of the paleoglenoid as a representative of native premorbid glenoid architecture which assumes no erosion of the paleoglenoid prior to development of the B2 morphology.³³ In contrast, in the study by Iannotti et al., premorbid glenoid version as measured by the glenoid vault model was only significantly more retroverted in C1 ($-19.0^\circ \pm 8.0^\circ$) and C2 ($-19.0^\circ \pm 8.0^\circ$) glenoids compared to A1 ($-5.1^\circ \pm 2.5^\circ$), A2 ($-5.3^\circ \pm 3.8^\circ$), B1 ($-6.5^\circ \pm 2.1^\circ$), B2 ($-8.3^\circ \pm 2.8^\circ$), and B3 ($-7.0^\circ \pm 3.2^\circ$) glenoids ($P < .002$).⁷

The increased detail and accuracy of 3D CT has also allowed for more precise assessment of orientations of glenoid bone loss as well as regional variations in glenoid bone density seen in B2 pathology.³⁴⁻³⁷ Three studies demonstrated B2 glenoid bone erosion to be positioned in a posterior inferior orientation.³⁴⁻³⁶ Using 3D CT to assess erosion patterns in B glenoids, Beuckelaers et al. showed mean erosion of 4.5 mm in B2 glenoids versus 3.5 mm in B1 ($P = .019$). The orientation of erosion was significantly different ($P = .004$) with B2 showing posterior inferior quadrant erosion at 113° from the mid superior glenoid compared to 132° in B1 glenoids (Figure 6).³⁴ In a similar assessment of preoperative 3D CT in 29 patients, Lombardo et al. found significantly more posterior and inferior bone loss in Walch B2 shoulders. Surgical planning also predicted greater risk of peg perforation in patients with greater bone loss, most commonly in B2 shoulders involving the central and posterior-inferior peg.³⁵ Lastly, Knowles et al. showed that the B2 wear pattern was directed posteriorly inferiorly with erosion starting on average 1.6 mm posterior to the glenoid center point and erosion lines were curved in 35% of cases. They also found the neoglenoid occupied on average 44% of the total glenoid area.³⁶ Variations of bone density with asymmetric glenoids were shown in a subsequent study of B2 glenoids with significantly higher density in the posterior quadrants compared with the anterior quadrants ($P < .001$). The neoglenoid exhibited significantly higher density compared with the paleoglenoid ($P < .001$).³⁷

Walker et al. recently demonstrated a trend of progression with B glenoids in glenohumeral OA. In this study of 65 patients, at least 2 consecutive CT scans of the shoulder a minimum of 2 years apart were analyzed using custom-designed 3D image reconstruction

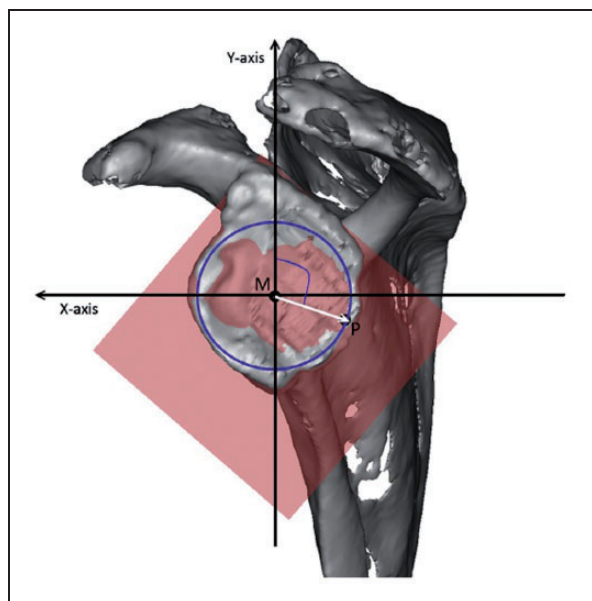


Figure 6. The orientation of the greatest erosion in B glenoid (reprinted with permission from Elsevier from Beuckelaers et al.³⁴).

software. At the time of latest follow-up CT, Type B glenoids more frequently progressed in comparison to Type A ($P < .001$). They showed 15 of the original 19 B1 glenoids progressed to B2 glenoids, 2 progressed to B3 glenoids, and only 2 remained in their original B1 classification. In contrast, 34 of the original 42 A1 glenoids did not progress and remained A1s. In addition, the odds of joint-line medialization occurring over time were 8.1 times higher for B-type glenoids than for A-type glenoids. For those glenoids that showed medialization, B-type glenoids showed more medialization over time than A-type glenoids.³⁸ In a follow-up study, Donohue et al. analyzed 190 CT scans in 175 patients who underwent TSA for glenohumeral OA to assess the relationship of glenoid morphology and rotator cuff pathology. Using 3D CT and respective 2D images, pathologic glenoid version and joint line, modified Walch classification and Goutallier classification were determined. High-grade posterior rotator cuff fatty infiltration (combined infraspinatus and teres minor) was seen in 16% B2 and 55% of B3 glenoids compared to 8% and 12% for A1 and A2 glenoids, respectively ($P < .001$). Higher fatty infiltration of the infraspinatus, teres minor, and combined posterior rotator cuff muscles was associated with increasing glenoid retroversion ($P < .05$), while higher fatty infiltration of all 4 rotator cuff muscles and combined posterior rotator cuff muscles was associated with increasing joint-line medialization ($P < .05$).³⁹

3D CT has provided vast information in comparisons to other imaging modalities by accurately characterizing

complex glenoid morphology and bone loss seen in the B2 glenoid, as well as rotator cuff pathology, which is useful as a preoperative planning tool in shoulder arthroplasty.

MRI Assessment

MRI carries value in assessment of the shoulder by permitting accurate assessment of the soft tissues surrounding the glenohumeral joint, particularly the rotator cuff, with elimination of ionizing radiation exposure. Yet, its utility in evaluation of glenohumeral OA has been examined far less than CT.

MRI has been shown to have more accurate assessment of glenoid bone loss and retroversion in comparison to plain radiographs.^{21,40} Raymond et al. showed in their assessment of 48 osteoarthritic shoulders a mean glenoid version of -14.3° on MRI and -21.6° on axillary radiographs. This mean difference, -7.36° , was statistically significant ($P < .001$). Intraobserver and interobserver reliability for MRI was shown to be of 0.96 and 0.9, respectively, while only 0.8 and 0.71, respectively, for axillary radiographs. Measured glenoid retroversion was greater in 73% of axillary radiographs.⁴⁰

Recently, Lowe et al. compared the accuracy of MRI to CT in assessment of glenoid version and Walch classification in 30 patients with glenohumeral OA. They found a mean glenoid version of -15.5° by CT and -18.6° by MRI ($P = .17$). Interobserver reliability was good for both modalities (CT, 0.73; MRI, 0.62), while intraobserver reliabilities were good to excellent for CT (range, 0.76–0.87) and good for MRI (range, 0.75–0.79). When assessing Walch classification, interobserver reliability for CT and MRI was only fair, whereas intraobserver reliability was moderate to good. Assessment of type A1, A2, and B1 was nearly equal between CT and MRI. More severe glenoid bone loss and dysplasia was less accurately assessed with MRI as significant divergence was seen with type B2 ($P = .001$) and C glenoids ($P = .03$). Specifically, MRI underrecognized type B2 glenoids (4% incidence vs 14% for CT), while the Type C glenoid was overidentified by MRI (22% incidence vs 13% for CT). The authors concluded that MRI is comparable to CT for the precise evaluation of glenoid version and identification of type A1, A2, and B1 glenoids, but inferior to CT for the identification of B2 and C glenoids.⁴¹

Although MRI appears to have superior accuracy in assessment of glenoid morphology compared to plain axillary radiographs, its utility compared to CT for assessment of more severe bone loss and retroversion, as seen in B2 glenoids, shows less reliability and accuracy.

Conclusion

The B2 glenoid poses significant challenges to surgeons both in its assessment and treatment.^{5–12,37} Plain x-rays are often the primary means of initial evaluation of glenoid pathology; however, their efficacy in detailed analysis of glenoid pathology compared to MRI and CT is significantly less comprehensive.^{18,21} CT, both standard 2D and 3D, offers greater assessment of glenoid morphology, yet standard 2D CT carries potential for inaccuracy if images are not appropriately corrected into the scapular plane.^{24,25,27} 3D CT has offered more detailed analysis of glenoid pathology^{6,7} and enhanced interpretation of premorbid and pathologic architecture of the B2 glenoid.^{33–37} MRI prevents exposure to ionizing radiation and its utility in assessment of symmetric glenoid wear shows no significant difference from CT, but it is notably weaker in identification of asymmetric glenoid wear seen in the B2 glenoid.⁴¹ The authors of this review routinely obtain preoperative CTs with utilization of 3D reconstruction for accurate assessment of glenoid pathology and presurgical implant templating. In conclusion, accurate preoperative identification of complex B2 glenoid pathology on imaging remains essential in planning and precise implant placement at the time of shoulder arthroplasty. Future research is needed to further understand pathologic progression of the B2 glenoid over time, including the etiology of posterior humeral head subluxation and how this leads to the development of posterior glenoid wear and biconcavity, and how changes in the rotator cuff muscles (fatty infiltration and/or atrophy) may contribute to this.

Declaration of Conflicting Interests

The author(s) declare the following potential conflicts of interest with respect to the research, authorship, and/or publication of the article: Royalties—Arthrex, DePuy-Synthes, Wright-Tornier, DJO; Consultant—DJO; Paid speaker/presenter—DJO; Financial/Material Support—JBJS, Wolters Kluwer Health—Lippincott Williams & Wilkins; Stock or stock options—Custom Orthopaedic Solutions; Board/Committee Member—AAOS, ABOS, ASES.

Funding

The author(s) received no financial support for the research, authorship, and/or publication of this article.

ORCID iD

Eric T Ricchetti  <https://orcid.org/0000-0002-4371-7998>

References

1. Kerr R, Resnick D, Pineda C, Haghghi P. Osteoarthritis of the glenohumeral joint: a radiologic-pathologic study. *Am J Roentgenol*. 1985;144(5):967–972.

2. Petersson CJ. Degeneration of the glenohumeral joint. An anatomical study. *Acta Orthop Scand*. 1983;54(2):277–283.
3. Gartsman GM, Brinker MR, Khan M, Karahan M. Self-assessment of general health status in patients with five common shoulder conditions. *J Shoulder Elbow Surg*. 1998;7(3):228–237.
4. Lo IKY, Litchfield RB, Griffin S, Faber K, Patterson SD, Kirkley A. Quality-of-life outcome following hemiarthroplasty or total shoulder arthroplasty in patients with osteoarthritis: a prospective, randomized trial. *J Bone Joint Surg Am*. 2005;87(10):2178–2185.
5. Walch G, Badet R, Boulahia A, Khoury A. Morphologic study of the glenoid in primary glenohumeral osteoarthritis. *J Arthroplasty*. 1999;14:756–760.
6. Bercik MJ, Kruse K II, Yalozis M, Gauci MO, Chaoui J, Walch G. A modification to the Walch classification of the glenoid in primary glenohumeral osteoarthritis using three-dimensional imaging. *J Shoulder Elbow Surg*. 2016;25(10):1601–1606.
7. Iannotti JP, Jun BJ, Patterson TE, Ricchetti ET. Quantitative measurement of osseous pathology in advanced glenohumeral osteoarthritis. *J Bone Joint Surg Am*. 2017;99(17):1460–1468.
8. Walch G, Moraga C, Young A, Castellanos-Rosas J. Results of anatomic nonconstrained prosthesis in primary osteoarthritis with biconcave glenoid. *J Shoulder Elbow Surg*. 2012;21:1526–1533.
9. Iannotti JP, Norris TR. Influence of preoperative factors on outcome of shoulder arthroplasty for glenohumeral osteoarthritis. *J Bone Joint Surg Am*. 2003;85-A(2):251–258.
10. Luedke C, Kissenberth MJ, Tolan SJ, Hawkins RJ, Tokish JM. Outcomes of anatomic total shoulder arthroplasty with B2 glenoids: a systematic review. *JBJS Rev*. 2018;6(4):e7.
11. Denard PJ, Walch G. Current concepts in the surgical management of primary glenohumeral arthritis with a biconcave glenoid. *J Shoulder Elbow Surg*. 2013;22(11):1589–1598.
12. Donohue KW, Ricchetti ET, Iannotti JP. Surgical management of the biconcave (B2) glenoid. *Curr Rev Musculoskelet Med*. 2016;9(1):30–39.
13. Neer CS II, Watson KC, Stanton FJ. Recent experience in total shoulder replacement. *J Bone Joint Surg Am*. 1982;64:319–337.
14. Scalise JJ, Codsí MJ, Brems JJ, Iannotti JP. Inter-rater reliability of an arthritic glenoid morphology classification system. *J Shoulder Elbow Surg*. 2008;17(4):575–577.
15. Nowak DD, Gardner TR, Bigliani LU, Levine WN, Ahmad CS. Interobserver and intraobserver reliability of the Walch classification in primary glenohumeral arthritis. *J Shoulder Elbow Surg*. 2010;19(2):180–183.
16. Knowles NK, Ferreira LM, Athwal GS. The arthritic glenoid: anatomy and arthroplasty designs. *Curr Rev Musculoskelet Med*. 2016;9(1):23–29.
17. Chan K, Knowles NK, Chaoui J, et al. Characterization of the Walch B3 glenoid in primary osteoarthritis. *J Shoulder Elbow Surg*. 2017;26(5):909–914.
18. Nyffeler RW, Jost B, Pfirrmann CW, Gerber C. Measurement of glenoid version: conventional radiographs

- versus computed tomography scans. *J Shoulder Elbow Surg.* 2003;12(5):493–496.
19. Aronowitz JG, Harmsen WS, Schleck CD, Sperling JW, Cofield RH, Sánchez-Sotelo J. Radiographs and computed tomography scans show similar observer agreement when classifying glenoid morphology in glenohumeral arthritis. *J Shoulder Elbow Surg.* 2017;26(9):1533–1538.
 20. Shukla DR, McLaughlin RJ, Lee J, Cofield RH, Sperling JW, Sánchez-Sotelo J. Intraobserver and interobserver reliability of the modified Walch classification using radiographs and computed tomography. *J Shoulder Elbow Surg.* 2019;28(4):625–630.
 21. Kopka M, Fourman M, Soni A, Cordle AC, Lin A. Can glenoid wear be accurately assessed using x-ray imaging? Evaluating agreement of x-ray and magnetic resonance imaging (MRI) Walch classification. *J Shoulder Elbow Surg.* 2017;26(9):1527–1532.
 22. Friedman RJ, Hawthorne KB, Genez BM. The use of computerized tomography in the measurement of glenoid version. *J Bone Joint Surg Am.* 1992;74:1032–1037.
 23. Rouleau DM, Kidder JF, Pons-Villanueva J, Dynamidis S, Defranco M, Walch G. Glenoid version: how to measure it? Validity of different methods in two-dimensional computed tomography scans. *J Shoulder Elbow Surg.* 2010;19(8):1230–1237.
 24. Bokor DJ, O'Sullivan MD, Hazan GJ. Variability of measurement of glenoid version on computed tomography scan. *J Shoulder Elbow Surg.* 1999;8(6):595–598.
 25. Bryce CD, Davison AC, Lewis GS, Wang L, Flemming DJ, Armstrong AD. Two-dimensional glenoid version measurements vary with coronal and sagittal scapular rotation. *J Bone Joint Surg Am.* 2010;92(3):692–699.
 26. Chalmers PN, Salazar D, Chamberlain A, Keener JD. Radiographic characterization of the B2 glenoid: the effect of computed tomographic axis orientation. *J Shoulder Elbow Surg.* 2017;26(2):258–264.
 27. Budge MD, Lewis GS, Schaefer E, Coquia S, Flemming DJ, Armstrong AD. Comparison of standard two-dimensional and three-dimensional corrected glenoid version measurements. *J Shoulder Elbow Surg.* 2011;20(4):577–583.
 28. Chalmers PN, Salazar D, Chamberlain A, Keener JD. Radiographic characterization of the B2 glenoid: is inclusion of the entirety of the scapula necessary? *J Shoulder Elbow Surg.* 2017;26(5):855–860.
 29. Kwon YW, Powell KA, Yum JK, Brems JJ, Iannotti JP. Use of three-dimensional computed tomography for the analysis of the glenoid anatomy *Shoulder Elbow Surg.* 2005;14(1):85–90.
 30. Scalise JJ, Bryan J, Polster J, Brems JJ, Iannotti JP. Quantitative analysis of glenoid bone loss in osteoarthritis using three-dimensional computed tomography scans. *J Shoulder Elbow Surg.* 2008;17(2):328–335.
 31. Scalise JJ, Codsí MJ, Bryan J, Iannotti JP. The three-dimensional glenoid vault model can estimate normal glenoid version in osteoarthritis. *J Shoulder Elbow Surg.* 2008;17(3):487–491.
 32. Ganapathi A, McCarron JA, Chen X, Iannotti JP. Predicting normal glenoid version from the pathologic scapula: a comparison of 4 methods in 2- and 3-dimensional models. *J Shoulder Elbow Surg.* 2011;20(2):234–244.
 33. Knowles NK, Ferreira LM, Athwal GS. Premorbid retroversion is significantly greater in type B2 glenoids. *J Shoulder Elbow Surg.* 2016;25(7):1064–1068.
 34. Beuckelaers E, Jacxsens M, Van Tongel A, De Wilde LF. Three-dimensional computed tomography scan evaluation of the pattern of erosion in type B glenoids. *J Shoulder Elbow Surg.* 2014;23(1):109–116.
 35. Lombardo DJ, Khan J, Prey B, Zhang L, Petersen-Fitts GR, Sabesan VJ. Quantitative assessment and characterization of glenoid bone loss in a spectrum of patients with glenohumeral osteoarthritis. *Musculoskelet Surg.* 2016;100(3):179–185.
 36. Knowles NK, Keener JD, Ferreira LM, Athwal GS. Quantification of the position, orientation, and surface area of bone loss in type B2 glenoids. *J Shoulder Elbow Surg.* 2015;24(4):503–510.
 37. Knowles NK, Athwal GS, Keener JD, Ferreira LM. Regional bone density variations in osteoarthritic glenoids: a comparison of symmetric to asymmetric (type B2) erosion patterns. *J Shoulder Elbow Surg.* 2015;24(3):425–432.
 38. Walker KE, Simcock XC, Jun BJ, Iannotti JP, Ricchetti ET. Progression of glenoid morphology in glenohumeral osteoarthritis. *J Bone Joint Surg Am.* 2018;100(1):49–56.
 39. Donohue KW, Ricchetti ET, Ho JC, Iannotti JP. The association between rotator cuff muscle fatty infiltration and glenoid morphology in glenohumeral osteoarthritis. *J Bone Joint Surg Am.* 2018;100(5):381–387.
 40. Raymond AC, McCann PA, Sarangi PP. Magnetic resonance scanning vs axillary radiography in the assessment of glenoid version for osteoarthritis. *J Shoulder Elbow Surg.* 2013;22(8):1078–1083.
 41. Lowe JT, Testa EJ, Li X, Miller S, DeAngelis JP, Jawa A. Magnetic resonance imaging is comparable to computed tomography for determination of glenoid version but does not accurately distinguish between Walch B2 and C classifications. *J Shoulder Elbow Surg.* 2017;26(4):669–673.